

Supporting Information

Rahimi et al. 10.1073/pnas.1419104111

SI Methods

Animals. All animal studies were approved by the Yale University Institutional Animal Care and Use Committee. The generation of PDK2/PDK4^{-/-} (DKO) mice was described previously (1). Wild-type mice were age-matched littermates of the DKO mice, which were generated on the C57BL6J background. Mice were housed in a temperature-controlled environment with a 12-h light/dark cycle and provided ad libitum access to standard chow (Harlan, diet 2018). At age 12 wk, groups of 24 male WT and 24 male DKO mice were fed 60% lard-based HFD (Research Diets, D12492) or maintained on the chow diet for 4 wk. For hyperinsulinemic-euglycemic clamp experiments, mice underwent jugular venous catheterization under isoflurane anesthesia. All animals were allowed to recover from surgery for at least 1 wk before experiments. Tissues were harvested at 17 wk of age with removal of food either 6 h or 16 h before killing.

Basal and Insulin-Stimulated Glucose Turnover Studies. Basal whole-body glucose turnover was assessed using [³-³H] glucose (HPLC-purified, Perkin-Elmer), infused at a rate of 0.05 μ Ci/min for 120 min. After the basal period, hyperinsulinemic-euglycemic clamps were conducted in conscious mice for 140 min, with a 3-min prime (22 mU/kg) followed by a continuous [3 mU/(kg-min)] infusion of human insulin (Novolin, Novo Nordisk), a continuous infusion of [³-³H] glucose (0.1 μ Ci/min), and a variable infusion of [1-¹³C] glucose (99% ¹³C enriched, 20 mg/dL) to maintain euglycemia (100–120 mg/dL). Plasma samples were obtained from the tail at 0, 30, 50, 65, 80, 90, 100, 110, 120, 130, and 140 min. The tail incision was made at least 2 h before the first blood sample was taken to allow for acclimatization, according to standard operating procedures. To measure tissue-specific glucose uptake, 10 μ Ci of 2-deoxy-D-[1-¹⁴C]-glucose (Perkin-Elmer) were injected as a bolus at 85 min. At the end of the clamp, mice were anesthetized with pentobarbital sodium injection (150 mg/kg), and harvested tissues were snap-frozen in liquid nitrogen. Plasma glucose was measured using a YSI 2700D glucose analyzer. Plasma levels of insulin and glucagon were measured using double-antibody RIA kits (Millipore). Biochemical analysis and calculations for the hyperinsulinemic-euglycemic clamps were performed as previously described (2).

Tissue Determination of V_{PDH}/V_{TCA} . V_{PDH}/V_{TCA} was estimated from the [4-¹³C] glutamate/[3-¹³C] alanine enrichment in quadriceps muscle (3). Fasting V_{PDH}/V_{TCA} was measured after a 2-h infusion of [1-¹³C] glucose (99% ¹³C enriched) at a rate of 1 mg/(kg-min), and insulin-stimulated V_{PDH}/V_{TCA} was measured at the end of the hyperinsulinemic-euglycemic clamp studies.

Determination of Fatty Acid Oxidation. Quadriceps skeletal muscle fibers were prepared according to a protocol as previously described (4). Briefly, a subsample of the dissected muscle of ~5 mg wet weight was immediately transferred onto a small Petri dish on ice containing 2 mL of ice-cold organ preservation solution (BIOPS) composed of 2.77 mM CaK₂ EGTA buffer, 7.23 mM K₂ EGTA buffer, 0.1 μ M free calcium, 20 mM imidazole, 20 mM taurine, 50 mM 2-(N-morpholino)ethanesulfonic acid hydrate (Mes), 0.5 mM DTT, 6.56 mM MgCl₂·6H₂O, 5.77 mM ATP, and 15 mM phosphocreatine (pH 7.1). The muscle sample was then gently dissected using forceps with sharp tips. To ensure complete permeabilization the fibers were incubated on a shaker at 4 °C in BIOPS solution containing 50 μ g/mL saponin for 30 min. Fibers were washed for 10 min at 4 °C in ice-cold mitochondrial respiration medium 5

[MiR05; 0.5 mM EGTA, 3 mM MgCl₂, 60 mM K-lactobionate, 20 mM taurine, 10 mM KH₂PO₄, 20 mM Hepes, 110 mM sucrose, and 1 g/L BSA essentially fatty acid free, adjusted to pH 7.1 (4)], and wet weight of the fibers was measured on a microbalance (Mettler Toledo). Subsequent respiration measurements were performed in MiR05 containing 2 mM carnitine at 37 °C using the high-resolution respirometer Oxygraph-2k (Oroboros).

All respirometric experiments were carried out in a hyperoxygenated Oxygraph chamber (250–400 μ M) to prevent any potential oxygen diffusion limitation to the muscle fiber bundle. A substrate-uncoupler-inhibitor titration protocol was used to assess fatty acid oxidation after addition of palmitoyl-CoA (50 μ M, all concentrations are final) with malate (2 mM) and saturating ADP concentrations (3 mM) present.

Determination of Oxidative Stress and Redox State in the Skeletal Muscle.

ROS production was measured by an enzyme-linked fluorescent technique whereby HRP uses Amplex Red (*N*-acetyl-3,7-dihydroxyphenoxazine) as an electron donor during the reduction of H₂O₂ to water. The resultant product, resorufin (7-hydroxy-3H-phenoxazin-3-one), is a highly colored and fluorescent compound and can be detected by a probe with a filter set of 563 nm and 587 nm excitation and emission wavelengths, respectively. Measurements were performed with an O2k-Fluorescence LED2 module (Oroboros Instruments) after 2-point calibration with H₂O₂ under constant stirring and temperature control. Mitochondria were isolated from quadriceps muscle of DKO mice. Briefly, the muscle was placed in 1 mL MiB06 containing 100 mM sucrose, 100 mM KCL, 50 mM Tris-HCl, 1 mM KH₂PO₄, 0.2 mM EFTA, and 0.5% fatty acid free BSA and cut into pieces. The sample was incubated for 2 min after addition of 1 mL protease solution (2 mg in 10 mL MiB06 buffer) and homogenized with a size 21 tissue grinder with glass pestle. After addition of 3 mL MiB06, the sample was centrifuged at 800 \times g for 10 min at 4 °C, and the supernatant was passed through two layers of cheesecloth and transferred to a new centrifuge tube. The sample was centrifuged at 10,000 \times g for 10 min at 4 °C, and the supernatant was discarded. The mitochondrial pellet was resuspended in 200 μ L buffer containing 280 mM sucrose, 5 mM Hepes, and 1 mM EGTA for determination of protein concentration. To assess maximum rates of ROS production from the ubiquinone-reducing site (site IQ) of complex I, isolated mitochondria (0.3 mg/mL) were incubated with ROS buffer containing 120 mM KCl, 5 mM Hepes, 5 mM K₂PO₄, 2.5 mM MgCl₂, 1 μ g/mL oligomycin, and 0.3% BSA with 50 μ M amplex red, 1 U.mL⁻¹ HPR, and 25 U.mL⁻¹ SOD for 5 min in the 2-mL chamber. Succinate (5 mM) was added, and the IQ ROS was determined as the rates sensitive to 4 μ M rotenone. To assess maximum rates of ROS production from complex I (NADH-ubiquinone oxidoreductase), isolated mitochondria (0.3 mg/mL) were incubated with ROS buffer and 50 μ M amplex red, 1 U.mL⁻¹ HPR, and 25 U.mL⁻¹ SOD for 5 min in the 2-mL chamber. Glutamate (5 mM) and 5 mM malate was added, and the ROS production was recorded after addition of 4 μ M rotenone.

Aconitase activity was measured by enzyme-based spectrophotometric assay (Cayman Chemical Company, item no. 705502), and NADPH oxidase activity was measured by ELISA (Wuhan EIAab Science Company, item no. E866m) in gastrocnemius muscle taken from overnight fasted WT and DKO mice. The high-energy intermediates, NADH and NAD⁺, as well as G6P, were measured in gastrocnemius tissue and extracted in a methanol, ammonium

acetate-based buffer by LC/tandem mass spectrometry, and values were normalized to an added internal standard, D₄-taurine. Tissues were rapidly acquired and in situ freeze-clamped and processed the same day for analysis by mass spectroscopy.

Metabolite Profiling. TAG in quadriceps muscle was extracted by the method of Bligh and Dyer (5) and measured enzymatically using the Triglyceride-SL reagent (Sekisui Diagnostics). Quadriceps DAG was extracted by homogenization in a buffer containing 20 mM Tris-HCl, 1 mM EDTA, 0.25 mM EGTA, 250 mM sucrose, and a protease inhibitor mixture (Roche). Homogenates were centrifuged at 100,000 × g for 60 min to separate the cytosolic and membrane fractions. DAG, acylcarnitine, ceramide, and long-chain acyl-CoA were analyzed by tandem mass spectrometry as described previously (6).

Measurement of Muscle Glycogen Content. Muscle glycogen content was assessed by amyloglucosidase digestion using the method of Passonneau and Lauderdale (7).

Assessment of Basal Metabolism in Mice. The Comprehensive Animal Metabolic Monitoring System (Columbus Instruments) was used to measure oxygen consumption, carbon dioxide production, caloric intake, energy expenditure, respiratory quotient, and activity. Mice were trained for 4 d (3 min/d) to run on a treadmill (Exer6M, Columbus Instruments).

Total RNA Preparation and Real-Time Quantitative PCR Analysis. RNA was extracted from frozen gastrocnemius muscle using RNEasy 96 kit (Qiagen), and then 1 μg of RNA was reverse-

transcribed into cDNA using the Quantitect RT kit (Qiagen). The abundance of transcripts was assessed by real-time PCR on a 7500 Real-Time PCR system (Applied Biosystems) with a SYBR Green detection system. Samples were run in duplicate for both the gene of interest and actin or GAPDH, and data were normalized for the efficiency of amplification, as determined by a standard curve included on each run. Primer sequences are available upon request.

Protein Expression. Tissue lysates were prepared using protease and phosphatase inhibitors (Roche) followed by determination of protein concentrations by Bradford assay (Thermo Fisher Scientific Inc.). Proteins were separated on a 4–12% Tris-glycine gel (Invitrogen) and transferred to a polyvinylidene difluoride membrane (Immobilon-P 0.45 μm, Millipore). Membranes were blocked with 5% milk and exposed overnight to primary antibodies: PDH-E1α pSer²⁹³ (Calbiochem), PDH-E1 α (Santa Cruz Biotechnology), total Akt and Akt pSer⁴⁷³ (Cell Signaling), PKC-θ (BD Transduction), Na-K ATPase (Abcam), and GAPDH (Santa Cruz Biotechnology).

PKC-θ Translocation. Membrane translocation of PKC-θ in quadriceps muscle from 6-h fasted mice was measured by immunoblotting of subcellular fractions as previously described (8).

Statistical Analysis. All data are expressed as mean ± SEM. Statistical significance was evaluated by two-tailed unpaired Student's *t* test or two-way ANOVA using GraphPad Prism. Differences with *P* values less than 0.05 were considered significant.

- Jeoung NH, Rahimi Y, Wu P, Lee WN, Harris RA (2012) Fasting induces ketoacidosis and hypothermia in PDHK2/PDHK4-double-knockout mice. *Biochem J* 443(3):829–839.
- Ayala JE, et al.; NIH Mouse Metabolic Phenotyping Center Consortium (2010) Standard operating procedures for describing and performing metabolic tests of glucose homeostasis in mice. *Dis Model Mech* 3(9–10):525–534.
- Alves TC, et al. (2011) Regulation of hepatic fat and glucose oxidation in rats with lipid-induced hepatic insulin resistance. *Hepatology* 53(4):1175–1181.
- Pesta D, Gnaiger E (2012) High-resolution respirometry: OXPHOS protocols for human cells and permeabilized fibers from small biopsies of human muscle. *Methods Mol Biol* 810:25–58.
- Bligh EG, Dyer WJ (1959) A rapid method of total lipid extraction and purification. *Can J Biochem Physiol* 37(8):911–917.
- Yu C, et al. (2002) Mechanism by which fatty acids inhibit insulin activation of insulin receptor substrate-1 (IRS-1)-associated phosphatidylinositol 3-kinase activity in muscle. *J Biol Chem* 277(52):50230–50236.
- Passonneau JV, Lauderdale VR (1974) A comparison of three methods of glycogen measurement in tissues. *Anal Biochem* 60(2):405–412.
- Choi CS, et al. (2007) Continuous fat oxidation in acetyl-CoA carboxylase 2 knockout mice increases total energy expenditure, reduces fat mass, and improves insulin sensitivity. *Proc Natl Acad Sci USA* 104(42):16480–16485.

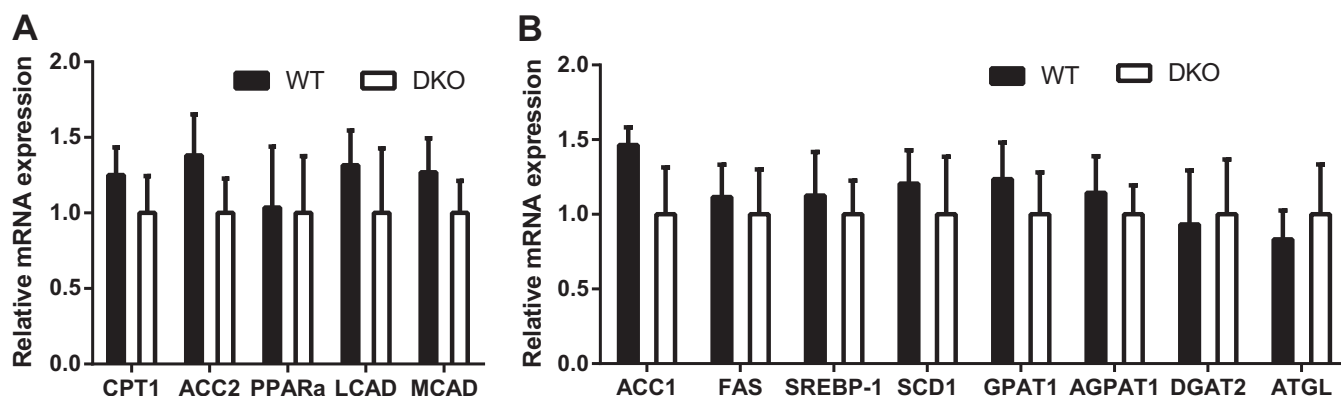


Fig. S1. Expression levels of key enzymes in fatty acid oxidation and lipid synthesis in the skeletal muscle of DKO mice. Levels of mRNA expression of enzymes in fatty acid oxidation (A) and lipid synthesis (B) in quadriceps taken from overnight fasted WT and DKO mice. *n* = 8 mice per group.

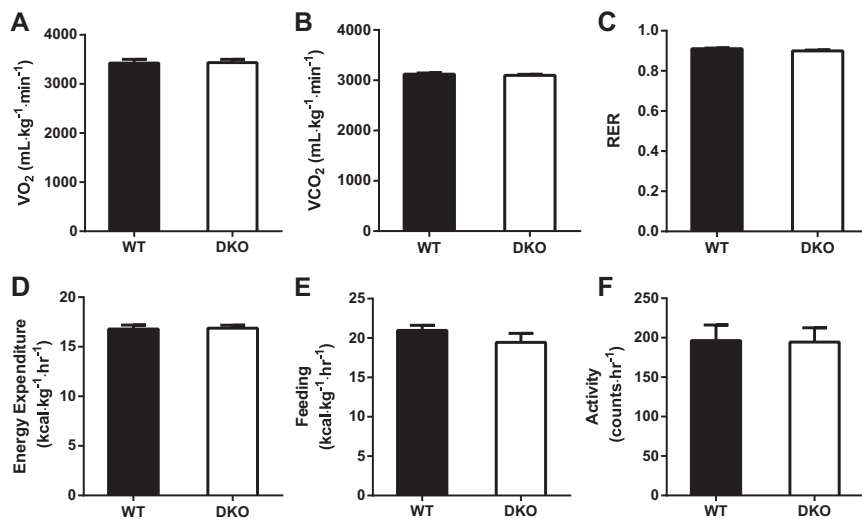


Fig. 52. Basal metabolic analysis of DKO mice. (A) Oxygen consumption, (B) carbon dioxide production, (C) respiratory quotient (RER), (D) energy expenditure, (E) food intake, and (F) activity measured in chow-fed WT and DKO mice by Animal Metabolic Monitoring System.

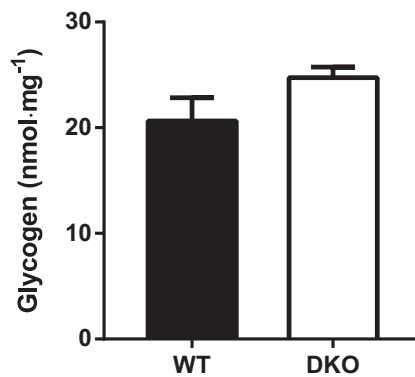


Fig. 53. Myocellular glycogen content in DKO mice. Glycogen content in 6-h fasted quadriceps taken from chow-fed WT and DKO mice. $n = 7$ mice per group.

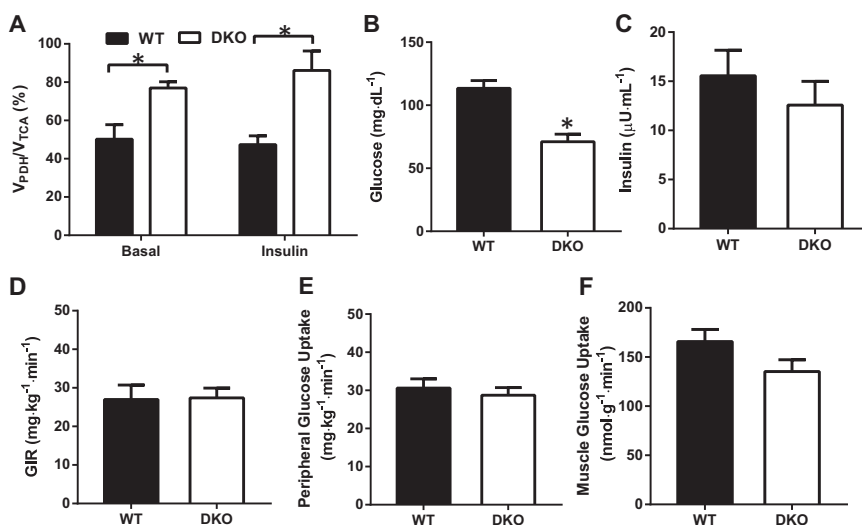


Fig. 54. Effect of 4-wk high-fat feeding on PDH flux and glucose uptake in the skeletal muscle of DKO mice. (A) Relative PDH flux (V_{PDH}/V_{TCA}) in the skeletal muscle WT and DKO after overnight fasting (basal) and at the end of the hyperinsulinemic-euglycemic clamp (insulin). Data are mean \pm SEM. $n = 6$ mice per group. (B) Fasting plasma glucose and (C) insulin concentrations, (D) glucose infusion rate to maintain euglycemia during the hyperinsulinemic-euglycemic clamp, and (E) insulin-stimulated peripheral glucose disposal during the hyperinsulinemic-euglycemic clamp. $n = 7$ –9 mice per group. (F) Insulin-stimulated glucose uptake in the quadriceps. Data are mean \pm SEM. $n = 6$ –8 mice per group.

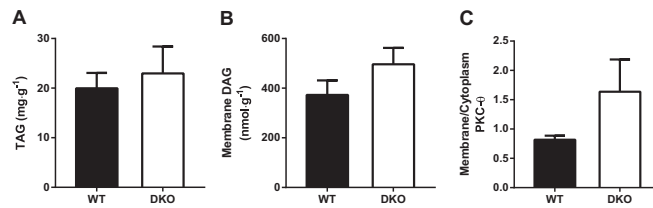


Fig. 55. Effect of 4-wk high-fat feeding on muscle-insulin resistance in WT and DKO mice. (A) Quadriceps TAG, (B) membrane DAG, and (C) membrane to cytosol ratio of PKC- θ in the skeletal muscle of WT and DKO mice after 6 h of fasting. Data are represented as mean \pm SEM. $n = 6$ –8 mice per group.

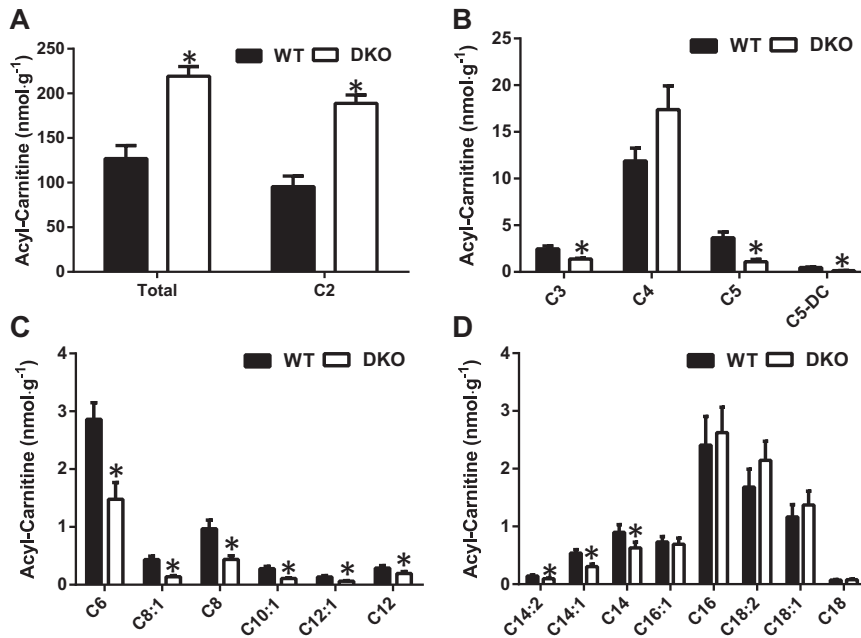


Fig. 56. Acylcarnitine profiling in the skeletal muscle of 8-wk HFD-fed DKO mice. (A) Total acylcarnitine and acetylcarnitine, (B) short-chain acylcarnitines, (C) medium-chain acylcarnitine, and (D) long-chain acylcarnitine levels in the quadriceps taken from 6 h fasted WT and DKO mice were measured by mass spectrometry. $n = 6$ –7 mice per group.

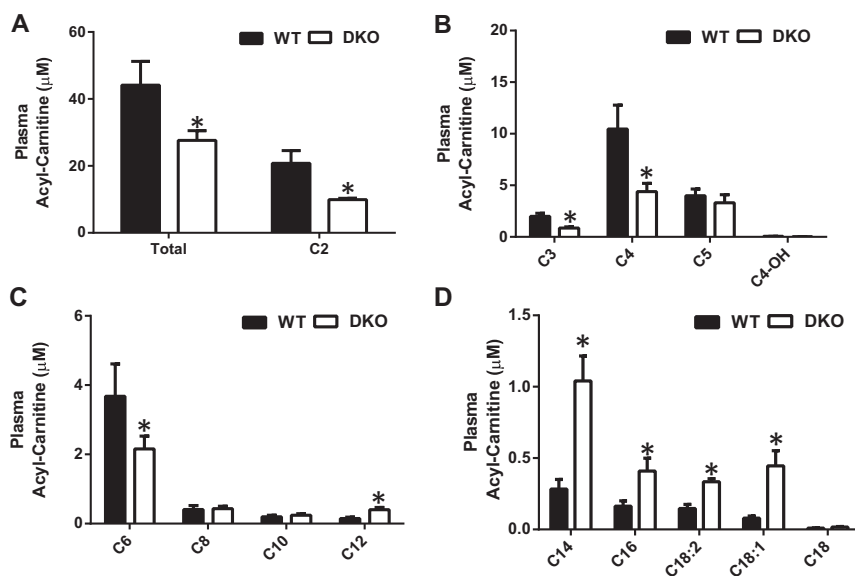


Fig. 57. Plasma acylcarnitine profiling in DKO mice. (A) Total acylcarnitine and acetylcarnitine, (B) short-chain acylcarnitines, (C) medium-chain acylcarnitine, and (D) long-chain acylcarnitine levels in plasma taken from overnight fasted WT and DKO mice were measured by mass spectrometry. $n = 6$ –8 mice per group.